

Design and Analysis of a Hybrid Mobile Robot Mechanism With Compounded Locomotion and Manipulation Capability

Pinhas Ben-Tzvi

Mem. ASME

e-mail: pinhas.bentzvi@utoronto.ca

Andrew A. Goldenberg

Fellow ASME

e-mail: golden@mie.utoronto.ca

Jean W. Zu

Fellow ASME

e-mail: zu@mie.utoronto.ca

Department of Mechanical and Industrial Engineering,
University of Toronto,
5 Kings College Road,
Toronto, ON, M5S 3G8, Canada

This paper presents a novel design paradigm as well as the related detailed mechanical design embodiment of a mechanically hybrid mobile robot. The robot is composed of a combination of parallel and serially connected links resulting in a hybrid mechanism that consists of a mobile robot platform for locomotion and a manipulator arm for manipulation. Unlike most other mobile robot designs that have a separate manipulator arm module attached on top of the mobile platform, this design has the ability to simultaneously and interchangeably provide locomotion and manipulation capability. This robot enhanced functionality is complemented by an interchangeable track tension and suspension mechanism that is embedded in some of the mobile robot links to form the locomotion subsystem of the robot. The mechanical design was analyzed with a virtual prototype that was developed with MSC ADAMS software. The simulation was used to study the robot's enhanced mobility characteristics through animations of different possible tasks that require various locomotion and manipulation capabilities. The design was optimized by defining suitable and optimal operating parameters including weight optimization and proper component selection. Moreover, the simulation enabled us to define motor torque requirements and maximize end-effector payload capacity for different robot configurations. Visualization of the mobile robot on different types of virtual terrains such as flat roads, obstacles, stairs, ditches, and ramps has helped in determining the mobile robot's performance, and final generation of specifications for manufacturing a full scale prototype. [DOI: 10.1115/1.2918920]

Keywords: mobile robot, hybrid mechanism, compounded locomotion and manipulation, virtual prototype, dynamic simulations

1 Introduction

The use of mobile robots is growing very rapidly in numerous applications such as planetary exploration, police operations (e.g., explosive ordnance disposal (EOD)), military operations (e.g., reconnaissance missions, surveillance, and neutralization of improvised explosive device (IED)), hazardous site exploration, and more. The use of unmanned ground vehicles (UGVs) in urban search and rescue (USAR) and military operations on urbanized terrain (MOUT) is gaining popularity because the mobile robots can be sent ahead or in place of humans, act on the surroundings with a manipulator arm or other active means attached to an arm, collect data about its surroundings, and send it back to the operator with no risks posed to humans.

In the past decade, new designs of mobile robots have emerged and were demonstrated by both academia and industry. Our work presents a new approach to mobile robot design for locomotion and manipulation purposes for a wide range of applications and practical situations. Typically, a mobile robot's structure consist of a mobile platform that is propelled with the aid of a pair of tracks, wheels, or legs, and a manipulator arm attached on top of the mobile platform to provide the required manipulation capability (neutralization of bombs or landmines, manipulation of hazardous materials, etc.). However, the presence of an arm limits the mobility. On the other hand, there are several designs of mobile robots that have pushed further the mobility state of the art such as

PackBot [1,2] and Chaos [3] including the ability to return itself when flipped over, but this may not be possible if the robot is equipped with a manipulator arm. This gap is bridged in our approach by providing a new mobile robot design that provides locomotion and manipulation capabilities simultaneously and interchangeably.

The new design is based on compounded locomotion and manipulation. The design approach is that the platform and manipulator arm are interchangeable in their roles in the sense that both can support locomotion and manipulation in several modes of operation as discussed in Sec. 4.2. Moreover, the design architecture enables the robot to flip over and continue to operate.

This paper is organized as follows. Section 2 provides a brief background to the field of mobile robots along with examples of existing types of design architectures. Section 3 introduces a conceptual function-oriented analysis that outlines a summary of existing issues related to tracked mobile robots, their related research problems, and proposed solutions. The new design resulting from the analysis of the issues identified is described in Sec. 4 along with presentation of several embodiments of the proposed design approach. To realize this design, a detailed mechanical design embodiment of the mechanically hybrid mobile robot is described in detail in Sec. 5 including the design of embedded and interchangeable track tension and suspension mechanism. In Sec. 6, the mechanical design is modeled and thoroughly analyzed in order to study the robot's functionality and optimize the design by defining suitable and optimal operating parameters such as required motor torques, manipulator end-effector capacity, etc.

Contributed by the Mechanisms and Robotics Committee of ASME for publication in the JOURNAL OF MECHANICAL DESIGN. Manuscript received July 26, 2007; final manuscript received January 25, 2008; published online May 20, 2008. Review conducted by Kwun-Lon Ting.

2 Background

Mobile robots were used for USAR activities in the aftermath of the World Trade Center (WTC) attack on September 11, 2001 [4,5]. The mobile robots were used mainly for searching of victims, searching paths through the rubble that would be quicker than to excavate, structural inspection, and detection of hazardous materials. In each case, small mobile robots were used because they could go deeper than traditional search equipment, could enter a void space that may be too small for a human or search dog, or could enter a place that posed great risk of structural collapse. Among the tracked robots that were used (such as Foster-Miller's Solem and Inuktun's Micro-Tracs and VGT), the capability was limited in terms of locomotion and mobility, and more so if one considers requirements of manipulation with an arm mounted on the mobile robot, which were not used at all. Some of the major problems with some of the robots used on the rubble pile searches were the robot flipping over or getting blocked by rubbles into a position from where it could not be righted or moved at all.

Increasingly, mobile robotic platforms are being proposed for high-risk missions for law enforcement and military applications (e.g., Iraq for IEDs), hazardous site cleanups, and planetary explorations (e.g., Mars rover). These missions require mobile robots to perform difficult locomotion and dexterous manipulation tasks. During such operations, loss of wheel traction, leading to entrapment, and loss of stability, leading to flipover, may occur, which results in mission failure.

Various robot designs with actively controlled traction [1,2,6–8], also called “articulated tracks,” were found to somewhat improve rough-terrain mobility. The mobility gains due to the articulated track mechanism yield a larger effective track radius for obstacle negotiation. Efforts are continuously made in designing robots that allow a wider control over center of gravity (COG) location [9] to produce robustness to effects attributed to terrain roughness. This was achieved by designing the robot with actively articulated suspensions to allow wider repositioning of the COG in real time. However, the implementations of such solutions may result in complex designs that may reduce robot’s operational reliability, and also increase its cost.

Mobile robot mechanical design architectures can be classified into several major categories such as tracked, wheeled, legged, wheel legged, leg wheeled, segmented, climbing, and hopping. The dozens of available mobile robots encompassing the aforementioned categories represent a fraction of the existing body of robotics research demonstrated by industry, research institutes, and universities. Therefore, due to the lack of consistent performance metrics reported by researchers, it would be very difficult to conduct performance comparisons between different robot architectures. A brief list of robots from each category is outlined as follows: (a) *tracked robots*: iRobot “Packbot” [1,2], Foster-Miller “Talon” [10], CMU “Gladiator” [11], Sandia “microcrawler” [12], ESI “MR-1 & MR-5” [13], and Remotec’s Andros series [6–8]; (b) *wheeled robots*: National Robotics Engineering Consortium “Spinner” [14], University of Minnesota “SCOUT” [15,16], Stanford “Stanley” [17], JPL “Inflatable Rover” [18], Draper “Throwbot” [19], EPFL “Alice” [20], and CMU “Millibot” [21]; (c) *legged robots*: Stanford “Sprawlita” [22], Draper “Bug2” [23], Draper “Ratbot” [23], Boston Dynamics “Big Dog” [24], and Frank Kirchner “Scorpion” [25]; (d) *wheel-legged robots*: Hirose Lab “Roller-Walker” [26], Lockheed Martin “Retarius” [27], JPL “ATHLETE” [28], EPFL “Octopus” [29], and EPFL “Shrimp” [30]; (e) *leg-wheeled robots*: University of Minnesota “SCOUT” [15,16], Draper “SpikeBall” [23], Boston Dynamics “RHex” [31], and CWRU “Mini-Whegs” [32]; (f) *segmented robots*: CMU “Millibots” [21], Draper “Throwbot” [23], Draper “HISS” [23], Draper “Rubble Snake” [23], and Draper “HMTM” [33]; (g) *climbing robots*: Stanford/JPL “Lemur” [34], Boston Dynamics “RiSE” [35], Clarifying Technologies “Clarifying Climber Robot”

[36], and iRobot “Mecho-gecko” [37]; and (h) *hopping robots*: JPL “Frog” [38], JPL “hopping robot” [39], Sandia “Self-Reconfigurable Minefield” [12], and Sandia “hopping robot” [12].

USAR and MOUT operations require high ground mobility capabilities for the mobile robot to operate in rough terrain such as in collapsed buildings, disaster areas, caves and other outdoor environments, as well as in man-made urbanized indoor and outdoor environments. In those missions, small UGVs are strictly limited by geometry since even the smallest obstacle can hinder mobility simply by physics. For instance, such a limitation occurs with wheeled mobile robots due to wheelbase and in legged robots due to leg step height, minimal contact area, etc. Another factor could be the result of actuator strength compared to the mobile robot mass.

Among the wide spectrum of mobile robot mechanisms available, wheeled architectures are the most common, and are universally accepted to be the most efficient means of locomotion over smooth terrain. The disadvantages of some wheeled robots are their limited obstacle negotiation capability, their available degrees of freedom of forward/reverse and steering limit, and their ability to handle mobility failures such as high centering. The maximum speed of wheeled robots is limited by rollover instability that is a function of steering curvature and terrain roughness. To solve the mobility problems of wheels, tracks are often used.

There are numerous good designs of tracked mobile robots such as PackBot [1,2], Remotec-Andros robots—Andros Mark V [6–8], Wheelbarrow MK8 Plus [40], AZIMUT [41], LMA [9], Matilda [42], MURV-100 [43], Helios Robots [44–47], Variable configuration VCTV [48], Ratler [49], MR-7 [13], NUGV [50], and Talon by Foster-Miller [10]. For instance, Helios VII robot from the Helios series robots of Hirose & Fukushima Robotics Laboratory provides some very good advances in terms of design and operation of tracked mobile robots for search and rescue missions [47]. Ideally, a robotic system that addresses all of the issues as analyzed and outlined in Sec. 3 in this paper would potentially yield a system with greater mobility and manipulation capabilities. As mentioned above, some legged robots [31,51] are also part of the scenarios assumed herewith, but we do not cover this area in this work. Our focus is on tracked mobile robots that are capable of providing locomotion as well as manipulation capabilities. Our goal is to present a new design that we derived based on a function-oriented analysis in order to address major design and operational issues of existing tracked mobile robots that also provide manipulation capabilities. We dedicated ample resources in developing a virtual prototype of the *entire robotic system* using ADAMS software to perform various dynamic simulations. The simulations were performed with the sole purpose to be used as a tool to study the robot, develop the design, optimize it, and define suitable operating parameters at different stages of the design and construction of the hybrid mobile robot.

3 Analysis of Issues and Related Research Problems and Proposed Solutions

A thorough review of the literature and discussions with users has assisted us in identifying major issues of design of mobile robots used in field operations. These issues are focused on robot functionality, and they have led us to our new design paradigm. The issues constitute a common denominator in the design of existing mobile robotic platforms. The issues are defined below along with proposed approaches for addressing them.

- (1) *Issue.* In current design architectures of mobile robots equipped with manipulation capability, the mobile platform and manipulator arm are two separate modules that are attachable to and detachable from each other. The platform and the arm have distinct functions that cannot be interchanged. Therefore, each module separately contributes to design complexity, weight, and cost. Also, the mass of the manipulator arm attached or folded on top of the mobile

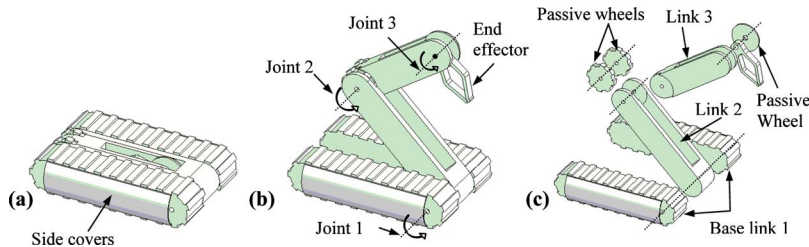


Fig. 1 (a) closed configuration, (b) open configuration, and (c) exploded view

platform is limited by the payload capacity of the mobile platform.

Approach to solution. The manipulator arm and the mobile platform are designed and packaged as one entity rather than two separate modules. The mobile platform is part of the manipulator arm, and the arm is part of the platform. Yet, the modules are attachable and detachable. The robot links' interchangeability to provide the functions of the mobile platform and manipulator arm requires fewer components (approximately 50% reduction in the number of motors) while at the same time the actuator strength capacity for manipulation purposes increases due to the hybrid nature of the mechanical structure. This approach may result in a simpler and more robust design, significant weight reduction, higher end-effector payload capability, and lower production cost.

- (2) *Issue.* In designs where the mobile robot includes a manipulator arm, it is mounted and folded on top. Therefore, the arm is exposed to the surroundings and hence is susceptible to breakage and damage especially when the mobile robot is flipped over.

Approach to solution. The arm and platform are designed as one entity, and the arm is part of the platform. The design architecture with the arm integrated in the platform eliminates the exposure to the surroundings when the arm is folded during motion of the mobile platform toward a target. As soon as the target is reached, the arm is deployed in order to execute desired tasks.

- (3) *Issue.* When operating over rough terrain, robots often reach positions from where they could not be righted or controlled further for a purpose. This requires special purpose or active means for self-righting in order to restart the robot's operation.

Approach to solution. In the new design architecture, the platform is *fully symmetric* even with the manipulator arm integrated, thus it can continue to the target from any situation with no need of additional active means for self-righting when it falls or flips over.

4 Description of the Design Concept

A new design paradigm was introduced in order to address the design problems mentioned above. The proposed approach is systematic and practical, and it addresses the overall system's operational performance. The proposed idea is twofold, and is described as follows.

- (1) The mobile platform and the manipulator arm are one entity rather than two separate and attached modules. Moreover, the mobile platform can be used as part of the manipulator arm and vice versa. Thus, some of the same joints (motors) that provide the manipulator's DOFs also provide the platform's DOFs, and vice versa.
- (2) The robot's adaptability is enhanced by "allowing" it to flip over and continue to operate instead of trying to prevent the robot from flipping over or attempting to return it (self-righteousness). When a flipover occurs, due to a fully symmetric design with the arm integrated, it is only required to

command the robot to continue to its destination from the current position. Furthermore, the undesirable effects of flipping over or free falling are compensated by a built-in dual suspension and tension mechanism that also allows effective terrain adaptability.

4.1 Concept Embodiment. To demonstrate the concept, Fig. 1 depicts a possible embodiment of the proposed idea. If the platform is inverted due to flipover, the *symmetric* nature of the design geometrical shape (Fig. 1(a)) allows the platform to continue to the destination from its new position with no need of self-righting. Also, it is able to deploy/stow the manipulator arm from either side of the platform.

The platform includes two identical base links (Link 1) with tracks (left and right), Link 2, Link 3, end effector, and passive wheels. To support the symmetric nature of the design, all the links are nested into one another. Link 2 is connected between the two base link tracks via Joint 1 (Fig. 1(b)). Passive wheels are inserted between Links 2 and 3 and connected via Joint 2 and another passive wheel is inserted between Link 3 and the end effector via Joint 3 (Fig. 1(c)). The passive wheels are used to support Links 2 and 3 when used for locomotion/traction. The passive wheels may be actively used for added mobility. Link 2, Link 3, and the end effector are nested into each other to allow complete symmetry of the platform's geometrical shape. They are connected through revolute joints and are able to provide continuous 360 deg rotation and can be deployed separately or together from either side of the platform. To prevent immobilization of the platform during a flipover scenario, rounded and pliable covers are attached to the sides of the platform, as shown in Fig. 1(a). The robot's structure allows it to be scalable and can be customized according to various application needs.

4.2 Modes of Operation. The links can be used in three different modes.

- (1) All links are used for locomotion to provide added level of maneuverability and traction.
- (2) All links are used for manipulation to provide added level of manipulability. The pair of base links can provide motion equivalent to a turret joint of the manipulator arm.
- (3) Combination of Modes 1 and 2: While some links are used for locomotion, the rest could be used for manipulation at the same time, thus the hybrid nature of the design architecture.

All three modes of operation are illustrated in Figs. 2–4. In the proposed design, the motor(s) used to drive the platform for mobility are also used for the manipulator arm to perform various tasks since the platform itself is the manipulator and vice versa. In other words, the platform can be used for mobility while at the same time it can be used as a manipulator arm to perform various tasks.

4.3 Maneuverability. Figure 2 shows the use of Link 2 to support the platform for enhanced mobility purposes as well as climbing purposes. Link 2 also helps to prevent the robot from being immobilized due to high centering, also enables the robot to

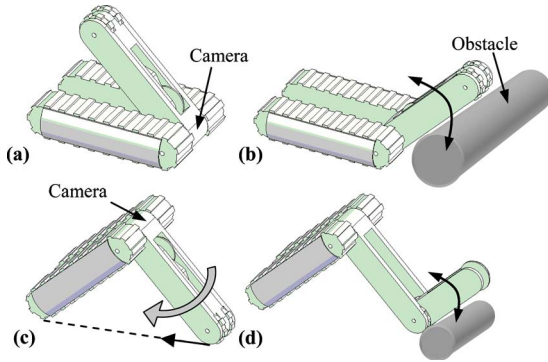


Fig. 2 Configurations of the mobile platform for mobility purposes

climb taller objects (Fig. 2(b)), and can help propel the robot forward through continuous rotation. Link 2 is also used to support the entire platform while moving in a tripod configuration (Fig. 2(c)). This can be achieved by maintaining a fixed angle between Links 2 and 1 while the tracks are propelling the platform. Configurations (a) and (c) in Fig. 2 show two different possibilities for camera use. Configuration (d) in Fig. 2 shows the use of Link 3 to surmount an object while Link 2 is used to support the platform in a tripod structure. The posture of the tripod configuration as shown in Fig. 2(c) can be switched by rotating Link 2 in a clockwise direction while passing it between the Base Link 1 tracks. This functionality is effective when it is necessary to rapidly switch the robot's direction of motion in a tripod configuration.

4.4 Manipulation. Figure 3 depicts different modes of configuration of the platform for manipulation purposes. While some links are used as platform for locomotion, others are simultaneously used for manipulation. Configuration (b) is similar to configuration (d) in terms of manipulation capabilities; however, configuration (d) is optimal for enhanced traction since the contact area between the platform and the ground is maximized. Configuration (b) is useful for increased maneuverability since the contact area between the platform and the ground is minimized. In all configuration modes for manipulation, while Links 2 and 3 are used for manipulation, the pair of base links can provide motion

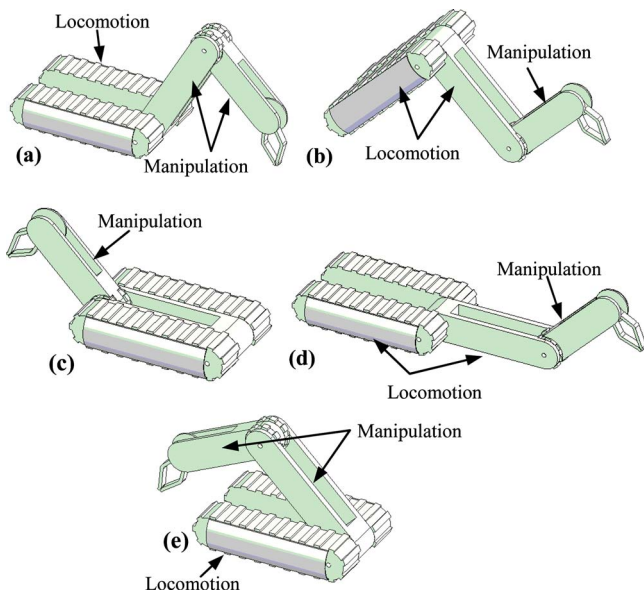


Fig. 3 Configuration modes for manipulation

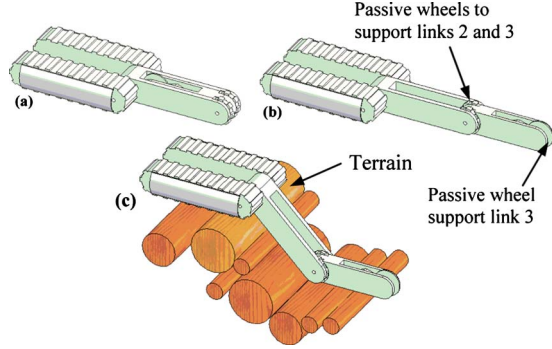


Fig. 4 Configurations for enhanced traction

equivalent to a turret joint of the manipulator arm. Further analysis on the stability gains of each configuration for manipulation as well as end-effector load capacity analysis of each configuration is discussed in the simulation results presented in Sec. 6.

4.5 Traction. For enhanced traction, Link 2, and if necessary Link 3 can be lowered to the ground level as shown in Figs. 4(a) and 4(b). At the same time, as shown in configuration (c), the articulated nature of the mobile platform allows it to be adaptable to different terrain shapes and ground conditions.

4.6 Additional Embodiments of the Concept. The main purpose of this section is to show that other possible embodiments of the concept may exist as well as to illustrate other locomotion means that could be used. Therefore, some of the design configurations shown in Fig. 5 may not be exactly realizable as shown. Figure 5 shows perspective schematic views of alternate embodiments of the hybrid mobile robot. Figure 5(a) shows the robot without tracks showing it with wheels. Figure 5(b) shows a perspective schematic view of an alternative hybrid mobile robot with the right and left base links aligned parallel to each other and joined at the front and back and the second link folds by the side of the base links and the third link folds inside the second link. Figure 5(c) shows a perspective schematic view of a further alternative hybrid mobile robot similar to Fig. 5(b) except that the third link folds by the side of the second link; and Fig. 5(d) shows a schematic view of a further alternative hybrid mobile robot with the right and left base links aligned parallel to each other and joined at the front and back, the second link being attached to one of the right and left base links, and the third link attached to the other of base links. The various configuration modes of mobility, manipulation, and traction as described in Figs. 2–4, respectively, can also be demonstrated by the alternative embodiments as described in Fig. 5.

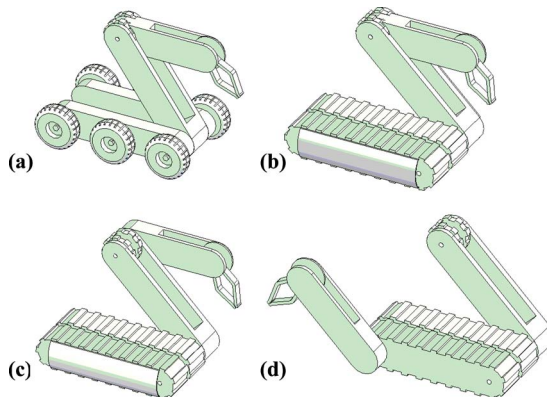


Fig. 5 Additional possible embodiments of the design concept

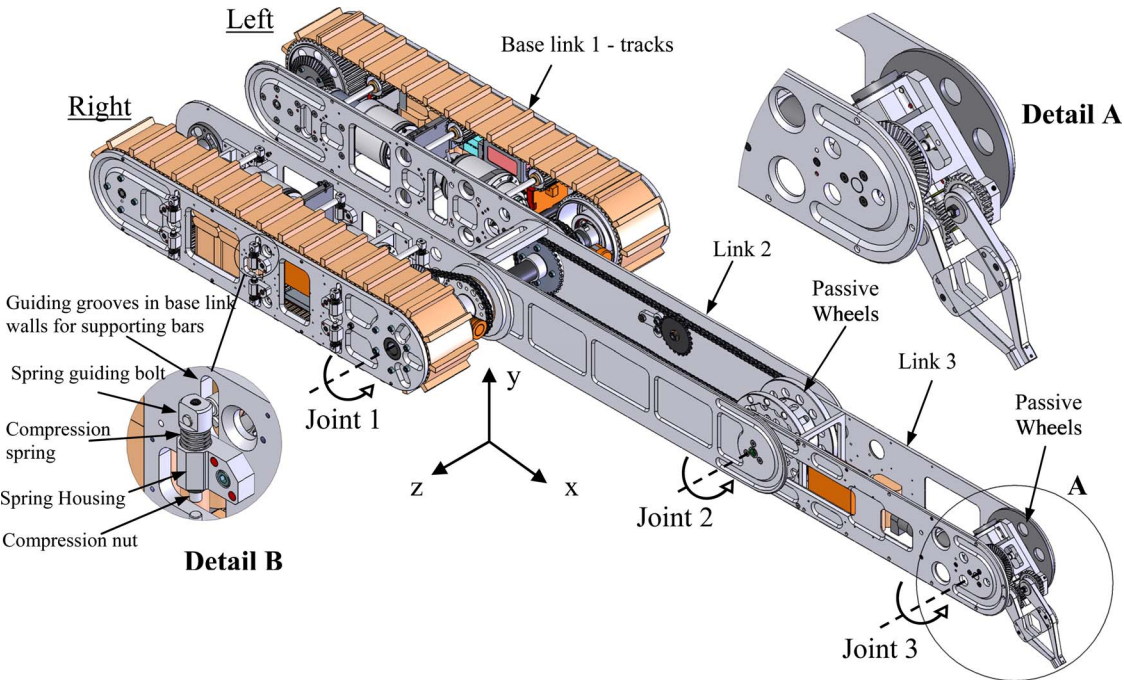


Fig. 6 Deployed-link configuration mode of the mobile robot

5 Mechanical Design Architecture

This section presents one implementation of the design concept as a case study. The presented case aims at describing the design structure as well as specific design issues and design novelties in detail. The case study provides a design solution selected from a range of alternatives that are described in Secs. 4.1 and 4.6. These solutions, generated from the conceptual function-oriented analysis, could be readily used in the development of various types and configurations of robots.

Figure 6 shows the complete mechanical design architecture of the mobile robot mechanism (with all covers removed). It embodies the conceptual design architecture described in Sec. 4.1, and includes the following design specifications and requirements: (i) design and package the manipulator arm and the mobile platform as one entity rather than two separate mechanisms; (ii) integrate the manipulator arm into the platform such that to eliminate its exposure to the surroundings; (iii) nest all robot links and the end-effector into each other to allow complete symmetry of the platform's geometry; (iv) provide the ability to deploy/stow the manipulator arm from either side of the platform; (v) integrate passive wheels into the robot joints in order to support the robot links when used for locomotion/traction; (vi) integrate each link with a revolute joint and to be able to provide continuous 360 deg rotation; (vii) attach rounded and pliable covers to the sides of the platform to prevent immobilization as well as to absorb some of the energy resulting from falling or flipping over of the robot; and (viii) embed interchangeable track tension and suspension mechanism in the mobile robot base links to form the locomotion subsystem of the robot.

The design includes two identical base link tracks (left and right), Link 2, Link 3, passive wheels, and end-effector mechanism (Fig. 6, Detail A). The two base links have identical orientations and they move together. This is achieved by fixing each of the base links to the ends of one common shaft. The common shaft is stationary and is located in Joint 1, as shown in Figs. 6 and 8. To support the symmetric nature of the design, all links are integrated into the platform such that they are nested into one another. Link 2 is connected between the left and right base link tracks via Joint 1 and is rotating about the main common shaft. Passive wheels are inserted between Links 2 and 3 and connected

via Joint 2 and another passive wheel is inserted between Link 3 and the end effector via Joint 3. The design also includes a built-in dual-operation track tension and suspension mechanism situated in each of the base link tracks and is described in detail in Sec. 5.3 and analyzed and simulated in Sec. 6.2. This section describes the platform drive system, arm joint design and integration of the arm into the platform, as well as several specifications of the robot based on a computer-aided design (CAD) detail design assembly that was used for the manufacturing of the prototype.

Along with the challenge and effort to realize the concept into a feasible, simple, and robust design, most of the components considered in this design are off the shelf. The assembly views show the platform/chassis design and the different internal driving mechanisms along with the description of the components used and their function. The closed configuration of the robot (Fig. 7—all links stowed) is symmetric in all directions x , y , and z . This design characteristic is extremely important for significantly enhancing locomotion ability. As shown in Fig. 7, rounded and pliable side covers are attached on the sides of the mobile robot to prevent immobilization when flipover occurs as well as to absorb some of the energy resulting from falling or flipping over events. Although the design is fully symmetric, for the purpose of explanation only, the location of Joint 1 will be taken as the reference point, and it will be called the front of the robot.

5.1 Motor Layout and Driving Mechanisms. The design includes four motors situated in the base links and two more in the space available in Link 3 for the gripper mechanism. Of the four motors located in the base links, two are situated at the back of each of the base links and the other two at the front (Fig. 8). All four motors at the base link tracks are identical Brushless DC Motors (BN34-25EU-02, available from Moog Components Group) with a rated power of 363 W and a continuous stall torque of 0.7 N m. The motor at the back of each base link provides propulsion to the track attached to that specific base link. The motion from each motor at the back is transmitted through a 1:32 ratio planetary servo gearbox (Series E60, available from Textron Fluid & Power) and a 1:2 ratio bevel gear in order to transfer the motion in a 90 deg angle as well as to amplify the torque capacity required for propelling the pulleys that drive the tracks. Both mo-

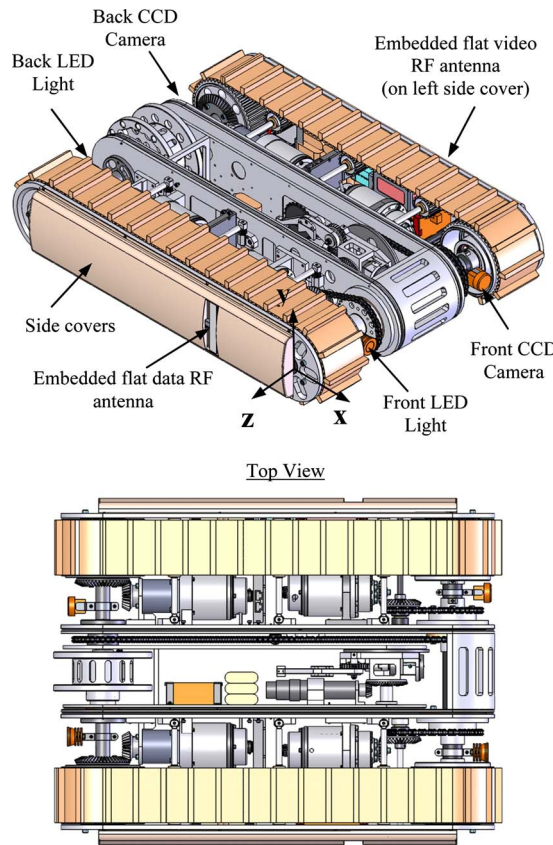


Fig. 7 Stowed-link configuration mode of the mobile robot (top/bottom covers removed)

tors at the back together provide the mobile robot translation and orientation in the plane of the platform. The motor at the front of each base link provides propulsion to one additional link. The motion is transmitted through a 1:120 ratio harmonic drive (CSF-20-120-2UH, available from Harmonic Drive Systems Inc.) and two additional transmission stages, namely, a 1:2 ratio bevel transmission followed by a 1:2.5 ratio chain and sprocket transmission in order to achieve greater torque capacities as required for Links 2 and 3 (Fig. 8). The motor at the front of the right base link propels Link 2 and the motor at the front of the left base link

propels Link 3 (Figs. 6 and 8). The required torque capacities were derived with the aid of the dynamic simulations as described in detail in Sec. 6, which helped us in selecting appropriate combination of components such as motors and gearheads. Each of the motors is equipped with a spring applied break (FSBR007, available from Inertia Dynamics) as well as a miniature optical encoder (E4 series, available from US Digital) for position and velocity control purposes. The overall location of the platform's COG is an important characteristic that affects the robot's tip-over stability. Therefore, the mechanical structure was derived such that motors and driving mechanisms for the tracks and all links are situated at the base to maintain the entire structure's COG closer to the ground.

The gripper mechanism along with its associated electronics and independent power sources are situated in the space available in Link 3. For the existing design, the gripper has two DOFs and hence two additional motors and gear systems. As for Links 2 and 3, the gripper submechanism is integrated such that it can provide continuous rotations about Joint 3 (Fig. 6, Detail A) and hence can be deployed from either side of Link 3. Rotation about Joint 3 is generated with a DC Micromotor (Series 3557-012C, available from Faulhaber Group) with an output power of 14.5 W and a continuous stall torque of 115 mN m, connected to a 1:246 ratio planetary gearhead (Series 38/2, available from Faulhaber Group) and a 1:3 ratio bevel gear. The open/close motion of the gripper is implemented with a flat brushless DC motor (EC45, available from Maxon Motor) with an output power of 12 W and a nominal torque of 22.8 mN m connected to a miniature 1:100 ratio Harmonic Drive (CSF-Mini Series Type 2XH-J, available from Harmonic Drive Systems Inc.) and a 1:30 ratio worm gear (Fig. 8).

5.2 Base Link 1 Tracks. The right and left base link tracks are each symmetric in all directions (x , y , and z) and identical in terms of the internal driving mechanisms although the mechanisms situated at the front each drives a different link.

In the center of each track, there is a solid self-tracking rib that fits into a guide located at the center of the main pulleys outer rim, as well as on all six planetary supporting pulleys, as shown in Fig. 9. This feature prevents the track from laterally sliding off, thus preventing the tracks from coming off the pulleys. In addition to the motors, as described in Sec. 5.1, all electrical hardware (such as batteries, controllers, drivers, electrical boxes, sensor boxes, Audio/Video and Data RF cards, gearheads, etc.) are situated in the left and right base link tracks. Other motors and associated electrical hardware for the gripper mechanism are situated in the space available in Link 3.

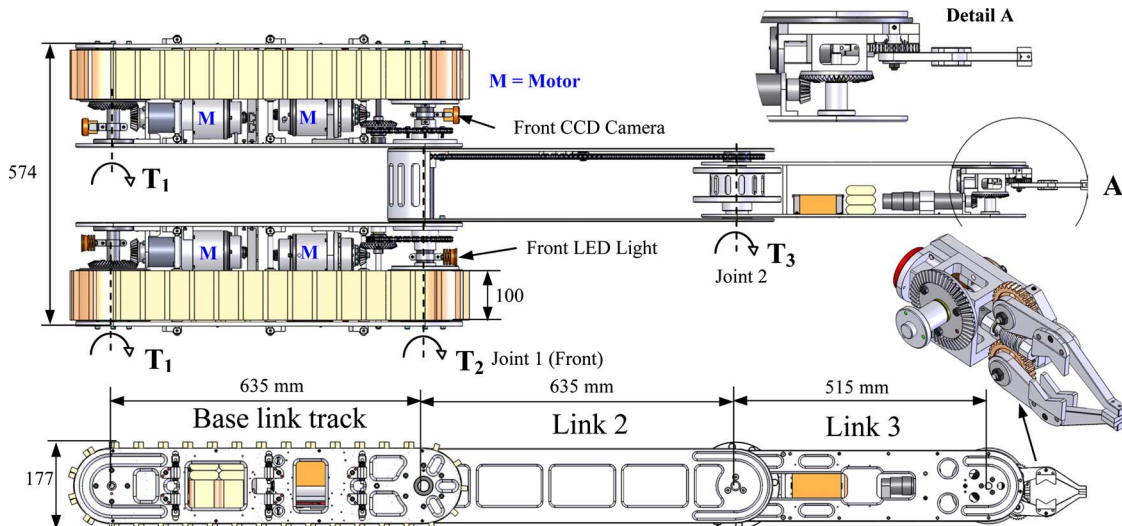


Fig. 8 Open configuration mode and general dimensions (front and top views—all covers removed)

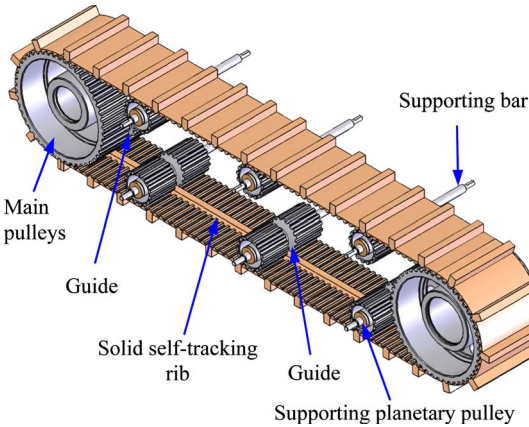


Fig. 9 Isometric view of base link track showing internal pulley arrangement

Other accessories typically found in mobile robots such as cameras, lights, and antennas are embedded in the platform. In other designs of mobile robots, these items typically stick out or protrude from the platform. In order to prevent their exposure to the surrounding and thereby eliminate risk of damage in cases where the robot flips over or falls, the charge-coupled device (CCD) cameras and light-emitting diode (LED) lights were embedded in the front and back of the left and right base link tracks, respectively, as shown in Fig. 7 and the top view in Fig. 8. Two special flat antennas are embedded in the right and left side covers for Data RF signals and Audio/Video RF signals, respectively (Fig. 7). The flat shape of the antennas and their location in the side covers maintain the symmetric nature of the entire hybrid platform and minimize the chance for loss of data or breakage of the antenna if it were to protrude vertically up.

5.3 Built-In Dual-Operation Track Tension and Suspension Mechanism. The arrangement of the supporting planetary pulleys is shown in Fig. 9. Each of the supporting pulleys is mounted on a supporting bar (Fig. 9) that is connected at each end to a compression spring (Fig. 6, Detail B). The ends of each supporting bar are guided through a groove on either side of the base link as shown in Detail B of Fig. 6. Therefore, each set of three planetary pulleys in the top and bottom of the left and right base link tracks is suspended by a 2×3 spring array. The purpose of the supporting pulleys is dual and provides two very important functions. While the bottom three supporting pulleys in each base link are in contact with the ground, they act as a suspension system. At the same time, the upper three supporting pulleys will provide a predetermined tension in the tracking system, as shown in Fig. 10. This dual operation track suspension and tension mechanism accounts for the symmetric nature of the design and operation of the mobile robot. In other words, if the platform is inverted, the three supporting pulleys that were used as suspension will act to maintain the tension in the tracks, while the other three pulleys that were used to provide tension in the tracks will act as

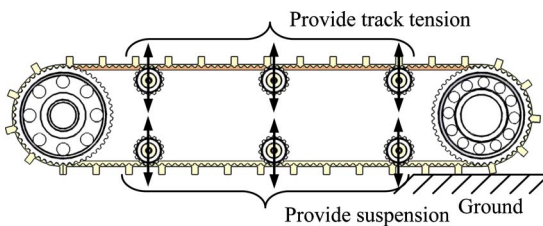


Fig. 10 Side view of base link track showing general pulley arrangement and track tension/suspension mechanism

Table 1 Robot design specifications

Total estimated weight (including batteries and electronics)	65 (kg)
Length (arm stowed)	814 (mm)
Length (arm deployed)	2034 (mm)
Width (with pliable side covers)	626 (mm)
Height (arm stowed)	179 (mm)

a suspension system. The required tension in the track belt and the suspension stroke can be preset by fastening or loosening the compression nuts (Fig. 6, Detail B). Another usage of the spring array is to absorb some energy resulting from falling or flipping, thus providing compliance to impact forces. Further discussion and analysis of this mechanism are provided in Sec. 6.2.

General design specifications of the robot are provided in Table 1. Photos of the hybrid mobile robot physical prototype in the close and open configurations are shown in Figs. 11(a) and 11(b). In order to support the reported mobility of this robot, a photo showing the prototype in the configuration illustrated in Fig. 13(a)(2) is shown in Fig. 11(c).

5.4 Robot Degrees of Freedom Coordination. The remote operating control unit (OCU) includes two control sticks in order to coordinate the robot degrees of freedom when generating the motions required for a given task. Of the four motors located in the base links, two are situated at the back of each of the base links and the other two at the front (Fig. 8). The motor at the back of each base link provides propulsion to the track attached to that specific base link. Both motors at the back together provide the mobile robot translation and orientation in the plane of the platform. The motor at the front of the right base link propels Link 2 and the motor at the front of the left base link propels Link 3 (Figs. 6 and 8). For the existing design, the gripper mechanism has two DOFs and hence two additional motors are located in the system.

The forward, backward, right turn, and left turn motions of the base link tracks are controlled by up, down, right, and left movements of the first control stick. The second control stick is used to control Links 2 and 3 degrees of freedom. A right movement of this control stick will generate a clockwise (CW) independent motion of Link 2 while a left movement of the stick will generate a counterclockwise (CCW) independent motion of Link 2. Simi-

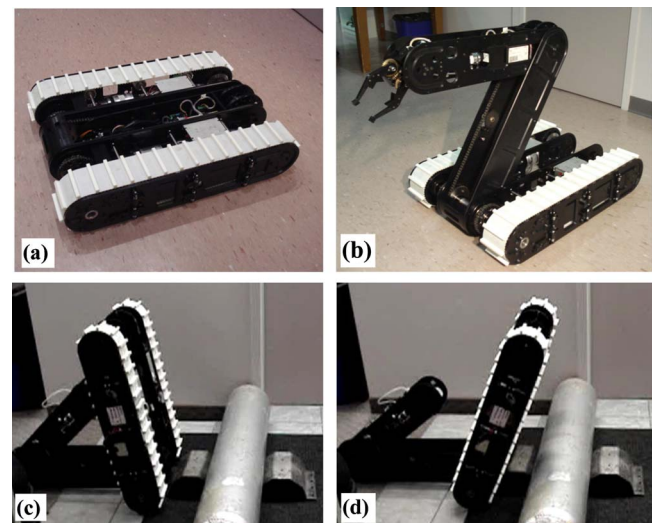


Fig. 11 A photo of the physical prototype: (a) stowed-link configuration mode, (b) open configuration mode, and (c) and (d) cylinder climbing configuration

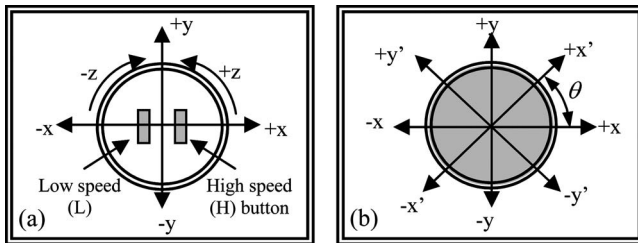


Fig. 12 (a) Control Stick No. 1 (C1) motion layout; (b) Control Stick No. 2 (C2) motion layout

larly, an up and down movement of the second control stick will generate an independent CW and CCW motion of Link 3, respectively. Furthermore, four diagonal movements of the second control stick (i.e., $+x'$, $-x'$, $+y'$, $-y'$ directions as shown in Fig. 12(b)) will generate simultaneous motions of Links 2 and 3 as follows.

- (i) Movement of the control stick in the $+x'$ direction will simultaneously move both Links 2 and 3 in the CW direction.
- (ii) Movement of the control stick in the $-x'$ direction will simultaneously move both Links 2 and 3 in the CCW direction.
- (iii) Movement of the control stick in the $+y'$ direction will simultaneously move both Links 2 and 3 in the CW and CCW directions, respectively.
- (iv) Movement of the control stick in the $-y'$ direction will simultaneously move both Links 2 and 3 in the CCW and CW directions, respectively.

The CW and CCW wrist motions of the gripper mechanism as well as the open and close motions of the gripper jaws are generated with a separate mode of the first control stick.

The first and second control sticks can be simultaneously operated by the operator in order to provide simultaneous motions of the tracks along with different motion combinations of Links 2 and 3, as explained above.

The above motion procedures are summarized in Fig. 12 and Table 2. Figure 12(a) shows the top view of Control Stick No. 1 (C1) with two switchable states as follows: (i) track motions—State 1 (S1); and (ii) gripper mechanism motions—State 2 (S2). Figure 12(b) shows the top view of Control Stick No. 2 (C2) with two coordinate systems x - y and x' - y' for Links 2 and 3 motions,

as specified in Table 2. The control angle θ in C2 provides speed variability to each of Links 2 and 3 when simultaneously operated.

6 Modeling and Dynamic Simulations of the Hybrid Robotic System

Dynamic simulations of the complete robotic system were performed in order to study its functionality and demonstrate its expected capability for design optimization purposes. The 3D mechanical design assembly that was developed with a CAD software was exported to and modeled in ADAMS software to perform motion simulations. The simulation experiments are accounting for the mass distribution of the robot (including batteries, motors, electronics, etc.), inertia properties and acceleration of the links, as well as contact and friction forces between the links and tracks and the ground.

When designing a mechanical system such as this hybrid robot, it was required to understand how various components interact as well as what forces those components generate during operation. We used ADAMS, commercial motion simulation software, to analyze the behavior of the entire robotic mechanical system. It allowed us to test virtual prototypes and optimize designs for performance, without having to build and test several physical prototypes. This dramatically reduced our prototype development time and cost.

The simulations enabled us to visualize and validate various robot mobility cases to study its functionality and hence optimize the design. The design optimization process involved weight distribution optimization, proper component selection (e.g., springs for track tension/suspension, motors, and gear ratios), etc. Weight distribution optimization was performed by identifying the optimal weight of each robot link (base links, Link 2, and Link 3) such that the robot's posture remained stable (tip-over stability) during the motion of the robot links while performing various locomotion and manipulation tasks. This was done by visualizing each task with the aid of the animations, as described in detail in Sec. 6.1, and changing the weight of each link as necessary until a stable posture was observed during the entire range of the link motion for a particular task. This procedure was repeated for several locomotion and manipulations tasks, as described in Secs. 6.1 and 6.4, respectively, until a common optimal combination of link weights was identified. The requisite for a flexible dynamics capability for the track system was addressed with ADAMS tracked vehicle (ATV) toolkit. A modus operandi using ADAMS and ATV toolkit was developed and used to model the tracks [52,53].

The data pertaining to each simulation performed were processed for the following specific major purposes that will be discussed in detail in subsequent subsections: (i) study the robot's mobility characteristics through animations of different possible tasks that require various locomotion and manipulation capabilities, (ii) analyze the suspension and track tension retention by examining the spring array force distributions, (iii) define each joint's torque requirements for different mobility tasks and select proper gear ratios and motors, and (iv) define maximum end-effector payload capacity for different robot configurations. Different types of terrains such as flat roads, obstacles, stairs, ditches, and ramps were created in a manner such that they could be easily changed according to different size and shape requirements.

6.1 Mobility Characteristics Analysis: Animation Results. To study the robot's functionality, the following simulations were performed: various manipulation scenarios (all three modes of operation as described in Sec. 4.2), random rotations of all links, traversing pipes of different diameters, climbing and descending rectangular obstacles with different link configurations, crossing ditches with different gap dimensions, climbing and descending stairs, flipping over due to a ramp obstacle, lifting tasks, and more. To illustrate, few of the above mentioned animation results

Table 2 Robot motion specifications

	FWD	BWD	Right	Left
Tracks motions	C1+S1 (+y) H/L	C1+S1 (-y) H/L	C1+S1 (+x) H/L	C1+S1 (-x) H/L
	Wrist CW	Wrist CCW	Gripper jaws open	Gripper jaws close
Gripper	C1+S2 (+y)	C1+S2 (-y)	C1+S2 (+z)	C1+S2 (-z)
	CW	CCW	CW/CCW	CCW/CW
Link 2 alone	C2 (+x)	C2 (-x)	N/A	N/A
Link 3 alone	C2 (+y)	C2 (+y)	N/A	N/A
Links 2+3	C2 (+x')	C2 (-x')	C2 (+y')	C2 (-y')

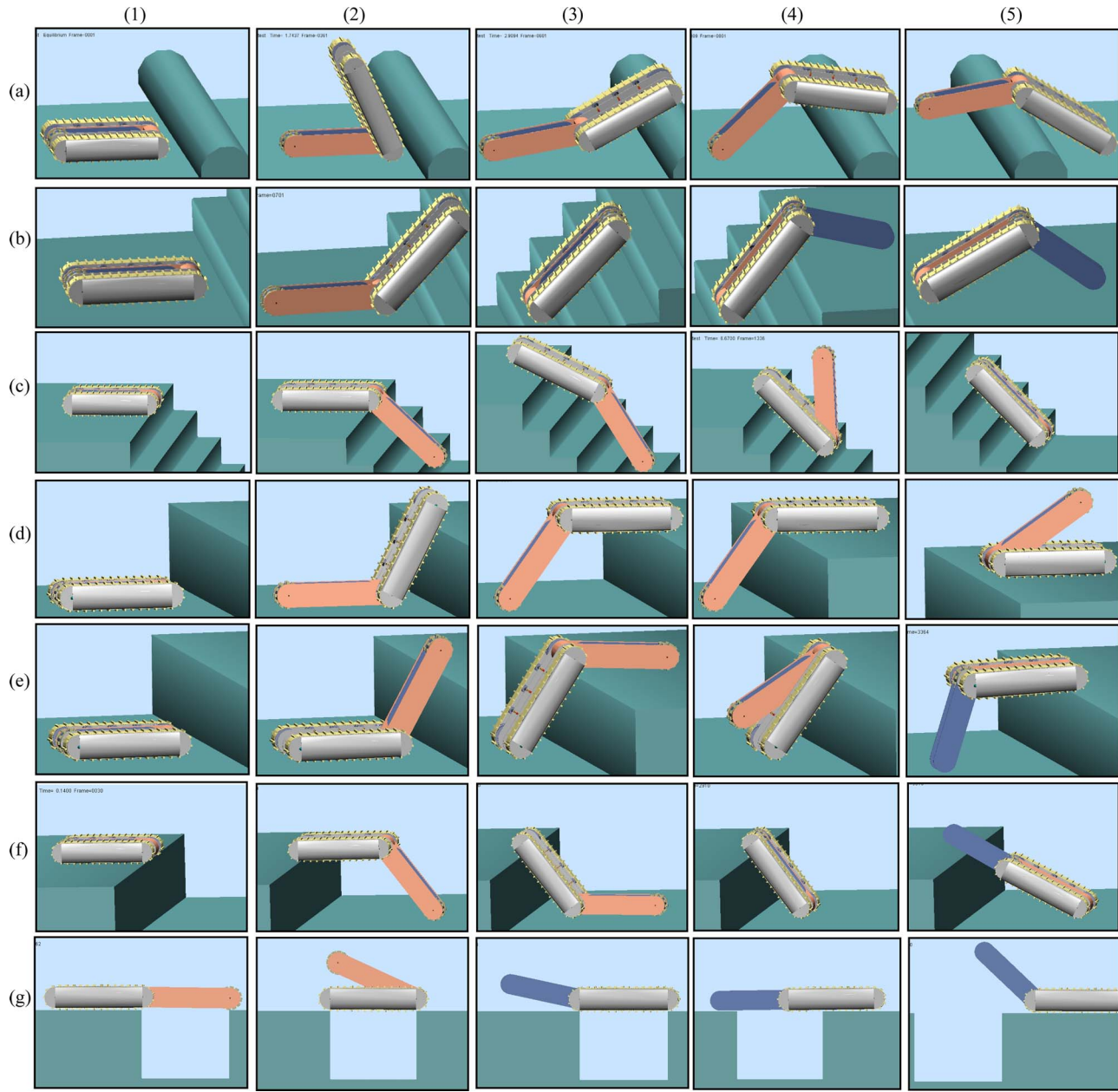


Fig. 13 Animation results: (a) surmounting cylindrical obstacles, (b) stair climbing, (c) stair descending, (d) step climbing with tracks, (e) step climbing with Link 2, (f) step descending, and (g) ditch crossing

are presented in Fig. 13. Each of the subfigures (a)–(g) represents several configuration steps (1)–(5) or motions that the different links along with the tracks need to undergo in order to accomplish each task or specific functionality. They are discussed as follows.

Surmounting cylindrical obstacles (Fig. 13(a)). The segmented and articulated nature of the robot's structure allows it to surmount large cylindrical obstacles such as pipes and tree logs with at least 0.4 m diameter. The base link tracks are deployed until they touch the obstacle (a)(1)–(3); at that point, the tracks propel the platform (a)(3) while at the same time they continue to rotate about Joint 1 (a)(4)–(5).

Stair climbing (Fig. 13(b)). The base link tracks are first deployed until they touch the stairs (b)(2); Link 2 is closed and the robot starts climbing with tracks (b)(3); at the end of the stairs, Link 3 opens (b)(4) to support the platform while the robot is in motion until configuration (b)(5); Link 3 rotates (until stowed be-

tween tracks) to lower the robot until the tracks fully contact the ground. Stairs with various riser/run dimensions can be climbed and descended.

Stair descending (Fig. 13(c)). Link 2 is deployed until it touches the stairs (c)(2); the robot advances until the entire platform is on the stairs (c)(3); Link 2 closes (c)(4); and the platform descends the stairs (c)(5).

Step climbing with tracks (Fig. 13(d)). The base link tracks are first deployed on the step (d)(2); Link 2 continues to rotate until the base link tracks adjust with the profile of the terrain (d)(3); the platform advances to accomplish the climbing process (d)(4) and Link 2 closes (d)(5). This climbing can also be accomplished with Link 3 by interchanging the roles of Links 2 and 3 (in this case, the back of the robot will be facing the step obstacle). Step heights of at least 0.5 m could be climbed and descended.

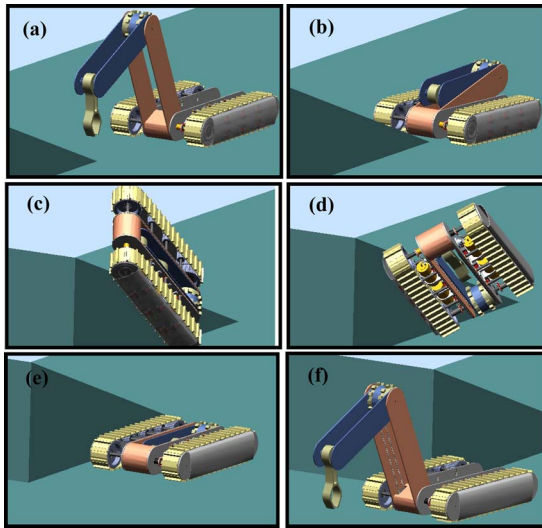


Fig. 14 Flipover scenario

Step climbing with Link 2 (Fig. 13(e)). This figure shows a series of configurations the robot needs to undergo in order to climb the step obstacle with Link 2 while Link 3 is deployed from the back to support the entire platform to complete the climbing process. This climbing can also be achieved with Link 3 by interchanging the roles of Links 2 and 3 (in this case, the back of the robot will be facing the step obstacle).

Step descending (Fig. 13(f)). Link 2 is deployed until it touches the ground to support the robot when advancing (f)(2), Link 2 rotates to lower the front of the platform (f)(3); Link 2 fully closes (f)(4); Link 3 opens to support the robot when moved forward (e); Link 3 rotates until closed to lower the robot until the tracks fully contact the ground.

Ditch crossing (Fig. 13(g)). Since the robot can deploy Link 2 from the front and Link 3 from the back (when all links are stowed), ditches up to 0.635 m in width can be easily traversed according to the following steps: from the back edge of the ditch, Link 2 is deployed (g)(1); the robot advanced until the front and back pulleys are supported by the ditch edges (g)(2); Link 2 closes and Link 3 opens from the back (g)(3); the robot continues its forward motion until the COG passes the front edge of the ditch while Link 3 prevents from the robot from falling into the ditch as long as the COG is before the front edge (g)(4)–(5).

The fully symmetric structure of the mobile robot along with its ability to sustain some forces resulting from falling or flipping over (due to its track suspension system and pliable rounded sides) can allow it to accomplish a mission requiring manipulation capabilities in spite of the fact that the robot flips over or falls due to an obstacle the robot could not avoid. Figure 14 shows several snapshots of a simulation showing a robot stowing its links before flipping over occurs and deploying them again from the other side of the platform after the robot flipped over.

6.2 Analysis of Track Tension and Suspension Mechanism.

These analyses aided in finding the optimal spring stiffness value for the dual tension-suspension mechanism. This was performed by visualizing the spring compression/expansion (with different stiffness values) to verify that it meets the allowable displacements for track tension and suspension purposes.

The graphs in Fig. 15 represent the force in each spring in the top and bottom spring arrays on each side of the platform (due to symmetry, each graph represents the force of the right and left springs in each base link). While the bottom supporting springs in each track contact the ground, they act as a suspension system for the platform. At the same time, the upper supporting springs exert forces upwards to maintain a predetermined tension in the track system. To illustrate this, Fig. 15 represents simulation results of the robot surmounting a small obstacle ($3 \times 4 \text{ cm}^2$) to observe how the springs react to obstacles situated between the planetary pulleys.

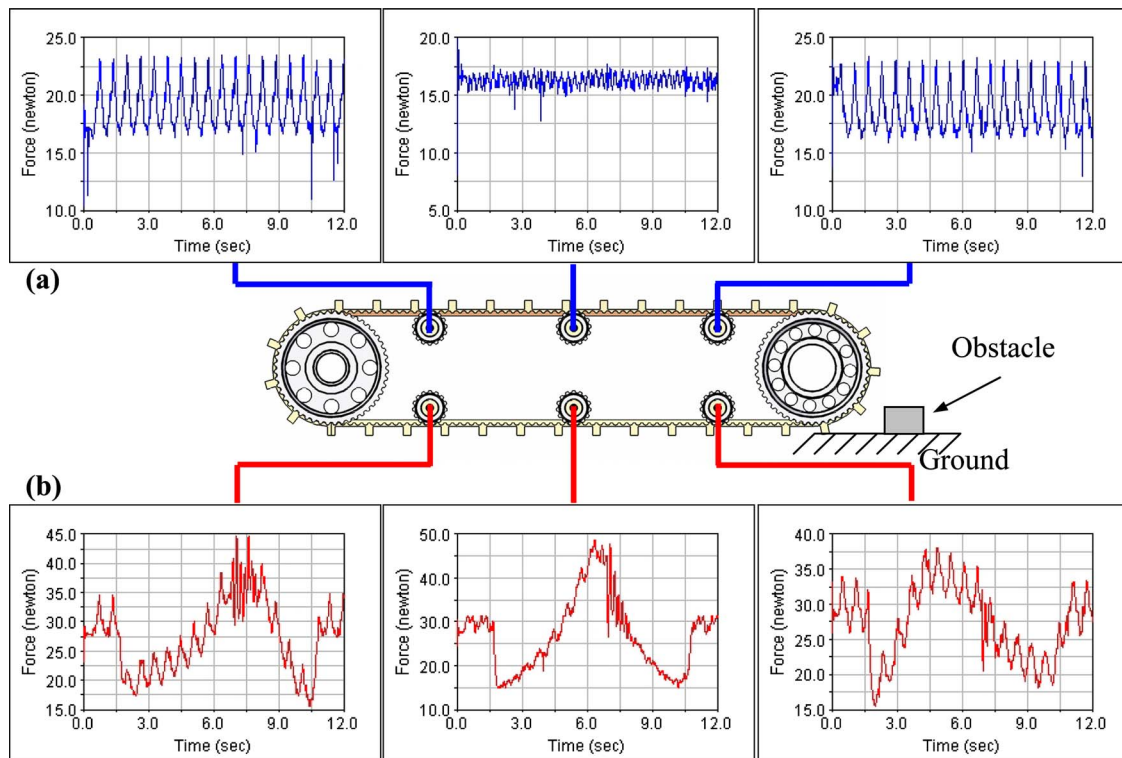


Fig. 15 Top ((a)—track tension) and bottom ((b)—suspension) spring array force distribution

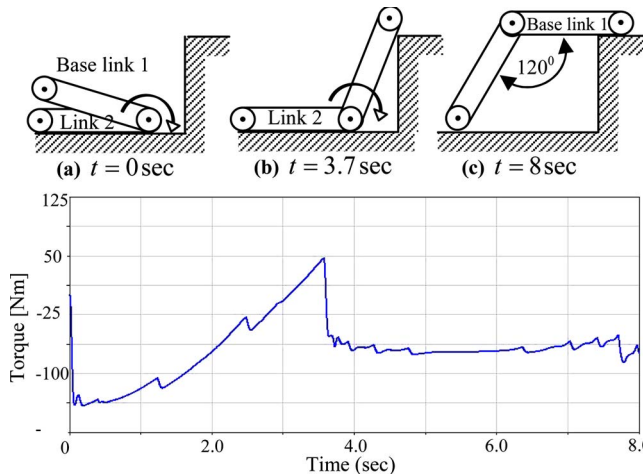


Fig. 16 Link 2 motor torque requirement—step obstacle climbing with tracks (via Joint 1)

From the top spring array force distribution (Fig. 15(a)), we observe that the average force in each spring is constant as expected since they support only the part of the track that does not touch the ground. In this case, the springs act to retain tension in the track. Also, the forces in the springs supporting the middle planetary pulley are generally smaller than those located off center, which is in agreement with the track shape characteristics due to its bending. Namely, the springs in the center are less compressed than those off center and hence generate less force. The forces are in the range 0–40 N as the installation compression of each spring was 8 mm and the optimal spring constant was found to be 5.19 N/mm.

From the bottom spring array force distribution (Fig. 15(b)), the force in each spring is fluctuating as expected since it supports the part of the track that touches the ground and hence in direct contact with the obstacle. The forces in all bottom springs are generally of equal range of magnitude since none of these springs are free to expand according only with the tracks pliability. In this case, the forces are greater than 40 N since the springs are compressed more than the installation compression value due to the ground's shape irregularities, which exert additional external forces on the tracks.

6.3 Analysis of Motor Torque Requirements. This section outlines the results of additional dynamic simulations performed in order to calculate the torque required in Joints T_1 , T_2 , and T_3 (Fig. 8) to propel the tracks, Link 2, and Link 3, respectively, for various mobility scenarios. Once the maximum torque requirement for each joint was evaluated, proper gear ratios and motors were selected.

Practically, the harshest operating conditions for each motor will dictate the motor's selection criteria. An analysis is performed for each motor in the system by generating torque plots for several mobility scenarios that require the largest torque capacity. Based on those torque plots, the maximum peak torque and its occurrence in a given range of motion are identified. The peak torque values define the maximum torque capacity necessary for each joint.

Figure 16 shows a series of motions the different links and the tracks need to undergo in order to climb a 0.5 m step height with the base link tracks and the torque required at every step of the motion. The angular velocity of Link 2 (30 deg/s) was used to identify the torque at every step of the motion with respect to the angle traveled by the link. According to the torque plot, the torque peak value for this case occurs at the beginning of the motion ($T_2=141.2$ N m at $t=0$). In another analysis similar to Fig. 16, if the climbing is performed with Link 2 (steps shown in Fig. 13(e)),

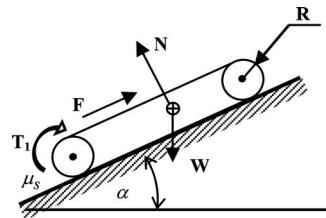


Fig. 17 Driving pulley motor torque requirement—inclined condition

a maximum torque value of $T_2=141.7$ N m was required.

Similar torque analysis procedure was performed to obtain Link 3 motor torque requirement (Joint 2) for different scenarios and was found to be $T_3=157$ N m. For symmetry reasons, we defined $T_2=T_3$ when selecting the motors and driving mechanisms for Links 2 and 3. In order to be able to generate the required torques, Lithium-ion batteries with high drain current capabilities as well as proper harmonic gearheads and brushless DC motors were incorporated in the design.

When the robot moves on a flat ground or a slope, the driving torque T_1 (Fig. 17) for a single track is determined based on the condition that slipping does not occur. Therefore, static friction coefficients were used to estimate the required driving force.

Equation (1) is used in order to estimate the driving force for a single track. Practically, vibrations and impacts occur in the driving system and there are random noises in real-time values of F_D .

$$F_D \geq \mu_s N + \frac{W}{2} \sin(\alpha) = \frac{W}{2} (\mu_s \cos \alpha + \sin \alpha) \quad (1)$$

To ensure incline motion conditions, the expression to estimate the torque can be written as follows:

$$T_1 \geq \frac{WR}{2} (\mu_s \cos \alpha + \sin \alpha) \left(\frac{1}{\eta_{\text{gear}} k_{\text{gear}} \eta_{\text{track}}} \right) \quad (2)$$

where F_D is the driving force of a single track (friction force), R is the outer radii of the track, W is the total weight, μ_s is the coefficient of static friction, η_{gear} is gear efficiency, k_{gear} is gear ratio (input to output rotational speeds), and η_{track} is track efficiency.

6.4 End-Effector Payload Capacity Analysis. The purpose of this simulation was to identify the maximum allowable end-effector load capacity of the platform with respect to various configurations by examining the COG vertical movement with respect to the ground, which indicates tip-over stability. The graph shown in Fig. 18 describes the change in the robot's COG position (in the vertical direction) with respect to linearly increasing load applied at the end effector. Among several simulation results based on various configurations, one possible optimal configuration for this purpose is shown in Fig. 18. The maximum end-effector load capacity was found at the instant when the COG position is greater than zero (dashed line in Fig. 18 graph), which indicates that the COG of the robot starts to move up vertically. According to the graph, the static load capacity with this configuration is ~ 77 kg. Practically, the maximum allowable torque capacity of Joints 1 and 2 will restrict the actual end-effector load capacity.

Possible selected configurations for manipulation are schematically presented in Fig. 19. Among the configurations shown in this figure, some other configurations can be generated in the range of the configurations shown, such as vertical or horizontal reach. For a given torque capacity in Joint 1, configuration (c) is optimal for maximum load capacity W_p due to its greater tip-over stability. In each of the configurations (b), (d), and (e) (depending on required level of mobility), an end-effector load of 18.3 kg is expected (with 157 N m torque capacity in Joints 1 and 2). This result is a direct consequence of the novel design architecture, namely, the

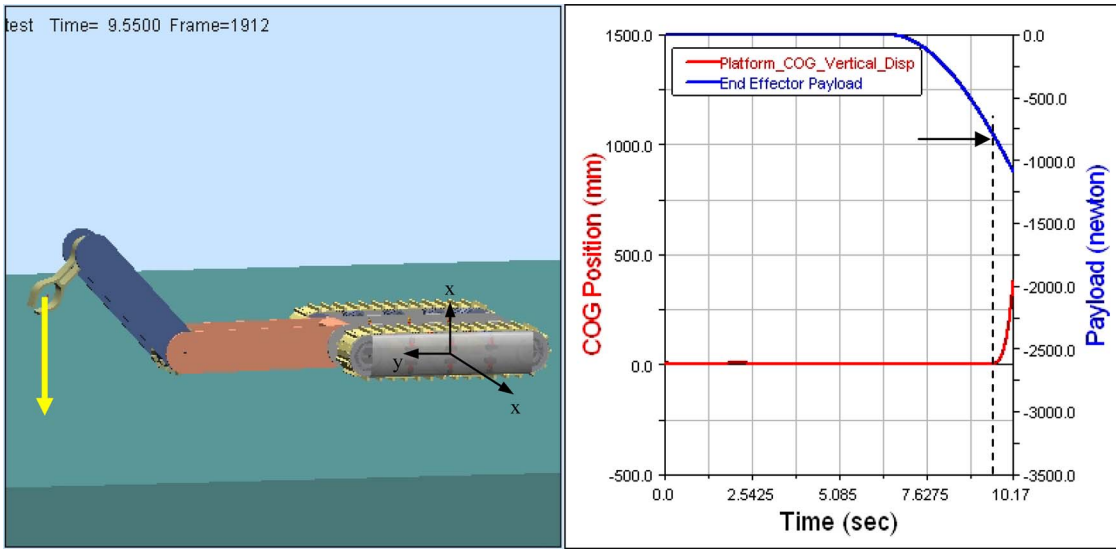


Fig. 18 Platform COG versus load capacity

hybrid nature of the platform and manipulator arm and their ability to be interchangeable in their roles.

7 Conclusion

The new mobile robot mechanical design paradigm presented in this paper was based on hybridization of the mobile platform and manipulator arm as one entity for robot locomotion as well as manipulation. The novel design was derived based on a conceptual function-oriented analysis, which addressed and summarized major issues of mobile robots in field operations. This design approach along with other design novelties and characteristics inherent to the robot presented provide solutions to various issues related to design of mobile robots operating on rough terrain and in hazardous environments as well as in man-made urbanized indoor and outdoor environments. The proposed approach is a systematic and practical design and development method that addressed the overall system's operational performance. These contributions toward the design approach should not only improve the designers' view of the design problem, but also allow novel design concepts with potentially better configurations. To model and analyze the overall robotic system, a virtual prototype was developed in ADAMS for multibody dynamic motion simulations of the complete robotic system. This has considerably reduced the prototype development time and cost while aiding with demonstrating the robot's expected functionality for design optimization purposes and derivation of optimal operating parameters. The derived param-

eters were used in the design and construction of a physical prototype.

Acknowledgments

This work was partially supported by Natural Sciences and Engineering Research Council of Canada (NSERC), grants held by Professor Andrew A. Goldenberg and Professor Jean W. Zu.

References

- [1] Yamauchi, B., 2004, "PackBot: A Versatile Platform for Military Robotics," Proc. SPIE, **5422**, pp. 228–237.
- [2] Frost, T., Norman, C., Pratt, S., and Yamauchi, B., 2002, "Derived Performance Metrics and Measurements Compared to Field Experience for the PackBot," in Proceedings of the 2002 PerMIS Workshop, Gaithersburg, MD.
- [3] Lewis, P. J., Flann, N., Torrie, M. R., Poulsom, E. A., Petroff, T., and Witus, G., 2005, "Chaos: An Intelligent Ultra-Mobile SUGV: Combining the Mobility of Wheels, Tracks, and Legs," Proc. SPIE, **5804**, pp. 427–438.
- [4] Carlson, J., and Murphy, R. R., 2005, "How UGVs Physically Fail in the Field," IEEE Trans. Rob. Autom., **21**(3), pp. 423–437.
- [5] Murphy, R. R., 2004, "Activities of the Rescue Robots at the World Trade Center From 11–21 September 2001," IEEE Rob. Autom. Mag., **11**(3), pp. 50–61.
- [6] White, J. R., Sunagawa, T., and Nakajima, T., 1989, "Hazardous-Duty Robots—Experiences and Needs," Proceedings of the IEEE/RSJ International Workshop on Intelligent Robots and Systems '89 (IROS '89), pp. 262–267.
- [7] White, J. R., Coughlan, J., Harvey, M., Upton, R., and Waer, K., 1989, "Taking Andros for a Walk," Nucl. Eng. Int., **34**(415), pp. 52–53.
- [8] Martens, J. D., and Newman, W. S., 1994, "Stabilization of a Mobile Robot Climbing Stairs," in Proceedings of the IEEE International Conference on Robotics and Automation, San Diego, CA, Vol. 3, pp. 2501–2507.
- [9] Goldenberg, A. A., and Lin, J., 2005, "Variable Configuration Articulated Tracked Vehicle," U.S. Patent No. 11/196,486.
- [10] TALON Mobile Robot, Foster-Miller. Available: <http://www.foster-miller.com/lemming.htm>.
- [11] Gladiator Mobile Robot, Robotics institute, available: <http://www.ri.cmu.edu>.
- [12] Sandia National Laboratories, available: <http://www.sandia.gov>.
- [13] MR-7 Tracked Mobile Robot, available: www.esit.com.
- [14] Bares, J., and Stager, D., 2004, "Expanded Field Testing Results From Spinner: A High Mobility Hybrid UGCV," Proceedings of the AUVSI Unmanned Systems 2004 Conference, Anaheim, CA.
- [15] Drenner, A., Burt, I., Dahlia, T., Kratochvil, B., McMillen, C. P., Nelson, B., Papanikopoulos, N., Rybski, P. E., Stubbs, K., Waletzko, D., and Yesin, K. B., 2002, "Mobility Enhancements to the Scout Robot Platform," Proceedings of the 2002 IEEE International Conference on Robotics and Automation, Washington, DC, pp. 1069–1074.
- [16] Drenner, A., Burt, I., Kratochvil, B., Nelson, B., Papanikopoulos, N., and Yesin, K. B., 2002, "Communication and Mobility Enhancements to the Scout Robot," Proceedings of the 2002 IEEE/RSJ International Conference on Intelligent Robots and Systems, Lausanne, Switzerland.
- [17] Russel, S., 2006, "DARPA Grand Challenge Winner," Popular Mechanics.
- [18] Behar, A., Matthews, J., Carsey, F., and Jones, J., 2004, "NASA/JPL Tumbleweed Polar Rover," Proceedings of the 2004 IEEE Aerospace Conference, Vol. 1, pp. 388–395.

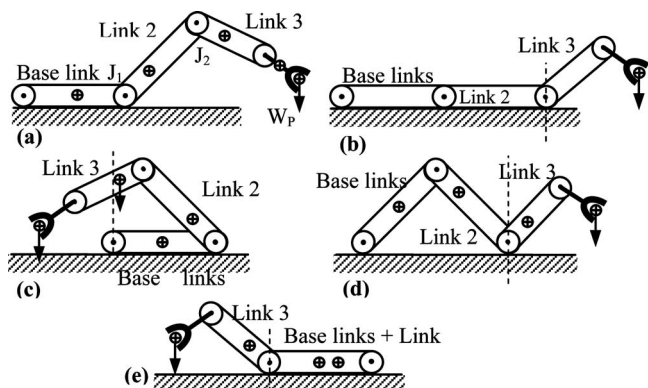


Fig. 19 Possible configurations for manipulation

- [19] Cleary, M. E., and Abramson, M., 2001, "Intelligent Autonomy for Small Throwaway Land Robots," *Proc. SPIE*, **4232**, pp. 421–427.
- [20] Caprari, G., Arras, K. O., and Siegwart, R., 2000, "The Autonomous Miniature Robot Alice: From Prototypes to Applications," *Proceedings of 2000 IEEE/RSJ International Conference on Intelligent Robots and Systems*, Vol. 1, pp. 793–798.
- [21] Brown, H. B., Jr., Weghe, J. M. V., Bererton, C. A., and Khosla, P. K., 2002, "Millibot Trains for Enhanced Mobility," *IEEE/ASME Trans. Mechatron.*, **7**(4), pp. 452–461.
- [22] Clark, J. E., Cham, J. G., Bailey, S. A., Froehlich, E. M., Nahata, P. K., Full, R. J., and Cutkosky, M. R., 2001, "Biomimetic Design and Fabrication of a Hexapedal Running Robot," in *Proceedings of 2001 IEEE International Conference on Robotics and Automation*, Vol. 4, pp. 3643–3649.
- [23] Draper Laboratory, available: <http://www.draper.com/>.
- [24] Buehler, M., Playter, R., and Raibert, M., 2005, "Robots Step Outside," *International Symposium on Adaptive Motion of Animals and Machines (AMAM)*, Ilmenau, Germany.
- [25] Klaassen, B., Linnemann, R., Spenneberg, D., and Kirchner, F., 2002, "Biomimetic Walking Robot SCORPION: Control and Modelling," *Rob. Auton. Syst.*, **41**(2–3), pp. 69–76.
- [26] Endo, G., and Hirose, S., 1999, "Study on Roller-Walker (Basic Experiments on Self-Contained Vehicle System)," *Proceedings of COE Workshop '99*, pp. 153–160.
- [27] Retarius Wheel-Legged Mobile Robot, Lockheed Martin, available: <http://www.lockheedmartin.com/>.
- [28] Wilcox, B. H., Litwin, T., Biesiadecki, J., Matthews, J., Heverly, M., Morrison, J., Townsend, J., Ahmed, N., Sirotta, A., and Cooper, B., 2007, "ATHLETE: A Cargo Handling and Manipulation Robot for the Moon," *J. Field Rob.*, **24**(5), pp. 421–434.
- [29] Lauria, M., Piguet, Y., and Siegwart, R., 2002, "Octopus—An Autonomous Wheeled Climbing Robot," in *Proceedings of the Fifth International Conference on Climbing and Walking Robots*, Professional Engineering Publishing Limited, Bury, UK.
- [30] Estier, T., Merminod, Y. C., Lauria, M., Piget, R., and Siegwart, R., 2000, "An Innovative Space Rover With Extended Climbing Abilities," in *Proceedings of Space and Robotics*, Albuquerque.
- [31] Saranli, U., Buehler, M., and Koditschek, D. E., 2001, "RHex: A Simple and Highly Mobile Hexapod Robot," *Int. J. Robot. Res.*, **20**(7), pp. 616–631.
- [32] Morrey, J. M., Lambrecht, B., Horchler, A. D., Ritzmann, R. E., and Quinn, R. D., 2003, "Highly Mobile and Robust Small Quadruped Robots," *Proceedings of the 2003 IEEE/RSJ International Conference on Intelligent Robots and Systems*, Vol. 1, pp. 82–87.
- [33] Larsen, R., and Kerrebrouck, P., 2003, "A High-Mobility Tactical Micro-Robot (HMTM) System," *Unmanned Systems Conference*, Baltimore, MD.
- [34] Kennedy, B., Agazarian, H., Cheng, Y., Garrett, M., Hickey, G., Huntsberger, T., Magnone, L., Mahoney, C., Meyer, A., and Knight, J., 2001, "LEMUR: Legged Excursion Mechanical Utility Rover," *Auton. Rob.*, **11**(11), pp. 201–205.
- [35] Autumn, K., Buehler, M., Cutkosky, M., Fearing, R., Full, R. J., Goldman, D., Groff, R., Provancher, W., Rizzi, A. A., Saranli, U., Saunders, A., and Koditschek, D. E., 2005, "Robotics in Scansorial Environments," *Proc. SPIE*, **5804**(1), pp. 291–302.
- [36] Clarifying Climber Robot, Clarifying Technologies, available: <http://www.clarifyingtech.com/>.
- [37] Sitti, M., and Fearing, R. S., 2003, "Synthetic Gecko Foot-Hair Micro/Nanostructures as Dry Adhesives," *J. Adhes. Sci. Technol.*, **17**(8), pp. 1055–1073.
- [38] Frog Hopping Robot, Jet Propulsion Laboratory, available: <http://www.jpl.nasa.gov/index.cfm>.
- [39] Fiorini, P., Hayati, S., Heverly, M., and Gensler, J., 1999, "A Hopping Robot for Planetary Exploration," *Proceedings of the 2004 IEEE Aerospace Conference*, Snowmass at Aspen, CO, Vol. 2, pp. 153–158.
- [40] Costo, S., and Molfino, R., 2004, "A New Robotic Unit for Onboard Airplanes Bomb Disposal," *35th International Symposium on Robotics ISR 2004*, Paris, pp. 23–26.
- [41] Michaud, F., Létourneau, D., Arsenault, M., Bergeron, Y., Cadrian, R., Gagnon, F., Legault, M. A., Millette, M., Paré, J. F., Tremblay, M. C., Lepage, P., Morin, Y., Bisson, J., and Caron, S., 2005, "Multi-Modal Locomotion Roéotic Platform Using Leg-Track-Wheel Articulations," *Auton. Rob.*, **18**(2), pp. 137–156.
- [42] Munkeby, S., Jones, D., Bugg, G., and Smith, K., 2002, "Applications for the MATILDA Robotic Platform," *Proc. SPIE*, **4715**, pp. 206–213.
- [43] HDE Manufacturing, Inc., 2006, "MURV-100: The EOD, SWAT, and WMD Robot System," available online: <http://www.hdemfg.com>.
- [44] Hirose, S., Fukushima, E. F., Damato, R., and Nakamoto, H., 2001, "Design of Terrain Adaptive Versatile Crawler Vehicle HELIOS-VI," *Proceeding of the IEEE/RSJ International Conference on Intelligent Robots and Systems*, Maui, HI, Vol. 3, pp. 1540–1545.
- [45] Hirose, S., Sensu, T., and Aoki, S., 1992, "The TAQT Carrier: A Pratical Terrain-Adaptive Quadruped Carrier Robot," *Proceedings of the IEEE/RSJ International Conference on Intelligent Robots and Systems*, Tokyo, pp. 2068–2073.
- [46] Hirose, S., Aoki, S., and Miyake, J., 1990, "Design and Control of Quadruped Crawler Vehicle HELIOS-II," *Proceedings of the Eight RoManSy Symposium*, Cracow, Poland, pp. 1–10.
- [47] Guarnieri, M., Debenest, P., Inoh, T., Fukushima, E., and Hirose, S., 2005, "Helios VII: A New Vehicle for Disaster Response, Mechanical Design and Basic Experiments," *Adv. Rob.*, **19**(8), pp. 901–927.
- [48] Iwamoto, T., and Yamamoto, H., 1990, "Mechanical Design of Variable Configuration Tracked Vehicle," *J. Mech. Des.*, **112**, pp. 289–294.
- [49] Purvis, J. W., and Klarer, P. R., 1992, "RATLER: Robotic All Terrain Lunar Exploration Rover," in *Proceedings of Sixth Annual Space Operations, Applications and Research Symposium*, Johnson Space Center, Houston, TX, pp. 174–179.
- [50] Blackburn, M. R., Bailey, R., and Lytle, B., 2004, "Improved Mobility in a Multi-degree-of-Freedom Unmanned Ground Vehicle (UGV)," *Proc. SPIE*, **5422**, pp. 124–134.
- [51] Full, R. J., and Koditschek, D. E., 1999, "Neuromechanical Hypotheses of Legged Locomotion on Land" *J. Exp. Biol.*, **202**, pp. 3325–3332.
- [52] Malik, S. M., Lin, J., and Goldenberg, A. A., 2006, "Virtual Prototyping for Conceptual Design of a Tracked Mobile Robot," *IEEE 2006 Canadian Conference on Electrical and Computer Engineering*, Ottawa, ON, Canada, pp. 2349–2352.
- [53] Malik, S. M., 2006, "Virtual Prototyping for Conceptual Design of Tracked Mobile Robots," M.S. thesis, Department of Mechanical and Industrial Engineering, University of Toronto, ON, Canada.